International Journal of Maritime Engineering

TIME-DOMAIN NON-LINEAR STRIP THEORY FOR SHIP MOTIONS

Y T Fan, University of Southampton, UK
P A Wilson, University of Southampton, UK

SUMMARY

A new implementation of strip theory is proposed based on the strip theory by Salvesen, *et al.* [1] and early work by Westlake and Wilson [2]. Compared with traditional strip theory, the main difference is that the calculation is carried out in the time domain. This makes it possible to cope with relatively large-amplitude motions and non-constant forward speed problems. At each time step, the exact underwater sections are extracted; the velocity potential is required to satisfy this instantaneous body boundary condition, therefore the added mass, damping coefficients and exciting forces are time variant, which produce a non-linearity. The diffraction force is added to work of Westlake and Wilson, and the results show the effect of diffraction force is significant.

NOMENCLATURE

$(0, 0, -H_G)$	Ship's centre of gravity in the calm water with respect to the coordinate system $o(x, y, z)$
(x_G, y_G, z_G)	Centre of gravity of the ship
$\bar{\phi}, \phi$	Velocity potential with respect to coordinate system $\bar{o}(\bar{x}, \bar{y}, \bar{z})$ and $o(x, y, z)$ respectively
$\bar{o}(\bar{x}, \bar{y}, \bar{z})$	Cartesian coordinate system fixed in space
η_0	Amplitude of the incident wave
$\hat{\phi}_k$	Two-dimensional velocity potentials
$\hat{n}_k$	Two-dimensional generalised normal vector
λ	Incident wave length
μ	Angle between the mean direction of ship motion and the direction of propagation of the incident wave
ω_0, ω_e	Incident wave frequency, frequency of encounter
φ_0, φ_1	Source potential, dipole potential
$\varphi_{2m}, \varphi_{2m+1}$	Multipole potentials
$\vec{\alpha}$	Displacement vector of a point on ship hull
$\vec{n}, \vec{n}$	Unit normal vector pointing out of the fluid domain in coordinate system $\bar{o}(\bar{x}, \bar{y}, \bar{z})$ and $o(x, y, z)$ respectively
ζ_j	Oscillatory motions of the ship
a, a_{2n}, a_{2n+1}	Conformal mapping coefficients
$A_{j,k}, a_{j,k}$	Three-, two-dimensional added mass coefficients
$B_{j,k}, b_{j,k}$	Three-, two-dimensional damping coefficients
F_j^I, F_j^D	Incident wave forces, diffraction forces
f_j^I, f_j^D	Sectional incident wave forces, sectional diffraction forces
F_j^R, F_j^S	Radiation forces, hydrostatic restoring forces
$I_{j,k}$	Moments of inertia of the ship
m	Mass of the ship
$M_{j,k}$	Generalised mass matrix for the ship
n_j, m_j	Generalised normal vectors
$o(x', y', z')$	Coordinate system fixed on the ship
$o(x, y, z)$	Equilibrium coordinate system moving with the ship
$P_{k,0}, P_{k,1}$	Expansion coefficient for source potential and dipole potential
$P_{k,2m}, P_{k,2m+1}$	Expansion coefficients for multipole potentials
U	Ship forward speed

1 INTRODUCTION

One of the crucially important aspects of ship design is the prediction of wave-induced ship motions and hydrodynamic loads in a realistic seaway.

Although the theoretical research can be traced as early as the work done by Froude [3] and Kriloff [4], the significant breakthrough was the strip theory developed by Korvin-Kroukovsky [5], which was the first motion theory suitable for numerical computations and had adequate accuracy for

engineering applications. Unfortunately inconsistencies in the mathematics were later found in this theory, particularly it did not satisfy the Timman-Newman relationships [6]. Modified versions of strip theory have since been proposed, of which, that developed by Salvesen, Tuck and Faltinsen [1] is mostly widely used in ship design. It provides satisfactory performance in the prediction of the motions of conventional ships as well as computational simplicity.

Conventional strip theory is deficient for low frequencies of encounter, and also for high ship speeds. Newman [7] developed a unified slender-body theory which relieved the frequency and speed restrictions that strip theory suffers and was successfully applied to seakeeping of ships [8]. Sclavounos [9] then extended it to the diffraction problem. This theory is further refined recently by Kashiwagi, *et al.* [10].

Since the the early 80's, due to the evolutionary advent of more powerful computers, seakeeping research on a complete three-dimensional numerical solution has blossomed. Unlike the two-dimensional theories (strip theory, unified slender-body theory, etc.), the three-dimensional methods can give detailed hydrodynamic pressure distributions over the hull surface, and can be applied to large structures which are no longer *slender* in all dimensions. Early efforts were contributed by Chang [11], and Inglis and Price [12, 13] who proposed a Green Function Method. By assuming the motions to be small and time harmonic, the numerical solution can be obtained by distributing the time-harmonic forward-speed free-surface Green function on the mean body surface and choosing their strengths to satisfy the necessary boundary conditions on this surface. Later developments are made by Wu and Eatock Taylor [14], and Chen, *et al.* [15].

An alternative three-dimensional method is the Rankine Panel Method which was initiated by Dawson [16]. Instead of using the Green function, Dawson distributed Rankine sources on the body surface as well as on the free surface which allows more general free surface conditions to be used. Nakos and Sclavounos [17, 18] applied this method to the seakeeping problem. The Rankine Panel Method removes the complexity of computing the free-surface Green function and the irregular frequency problem in the Green Function Method. The drawback is that it requires many more panels than the Green Function Method and its stability is a major question.

While deriving the above frequency-domain methods, it was assumed that body motions were steady and sinusoidal in time. Therefore, those methods are not applicable to unsteady transient problems. Based on the early work of Finkelstein [19], Wehausen [20] provided the rigorous theoretical basis for the using time-domain Green function to solve unsteady ship motion problems at zero forward speed. Computations directly from this method were presented by Yeung [21] and Newman [22] for two-dimensions. Three-dimensional computations were then given by Beck and Liapis [23] for the zero speed radiation problem, and by King, *et al.* [24] for the non-zero forward speed seakeeping problem. The Time-Domain Green Function Method is found much more effective than the Frequency-Domain Green Function Method in the case that the body's forward speed is included. This is because the forward-speed frequency-domain Green function is very complicated and extremely difficult to calculate, whilst the forward-speed time-domain Green function retains the same relatively simple form as zero-speed frequency-domain Green function regardless of the body's velocity. The time-domain Rankine Panel Method was developed by Nakos, *et al.* [25].

A important advantage of time-domain methods is that they could be extended to solve large-amplitude motions by applying the exact body boundary condition on the instantaneous wetted hull surface. If the free-surface boundary condition remains linearised, this body-exact approach is time variant linear. An example of Body-Exact Time-Domain Green Function Method was given by Lin and Yue [26]. Meanwhile, Kring, *et al.* [27], Sclavounos, *et al.* [28], and Huang and Sclavounos [29] have given the examples of Body-Exact Time-Domain Rankine Panel Method.

The three-dimensional methods have been proved to give, in general, better agreement with experimental data, however, strip theory is still the most popular theory. This is because strip theory has distinctive benefits compared with three-dimensional methods. Firstly, it is reliable and requires much less numerical calculation than the three-dimensional methods, whilst its accuracy is quite reasonable for engineering applications. Secondly, strip theory just requires the offset data on ship sections, while the three-dimensional methods need the three-dimensional ship surface data. This makes strip theory more feasible for the analysis of the seakeeping performance in the initial ship design stage.

In the last decade, strip theory seems to be neglected, all the efforts have been focused on the development of time-domain three-dimensional methods, yet few works on refining strip theory can be found. Beck and Reed [30] estimated that probably 80 percent of all the current calculations related to ships with forward speed are still made by using strip theory. In this paper, the traditional strip theory is extended to deal with large-amplitude ship motions and non-constant forward speed problems.

Generally the steady-state time-harmonic ship motions (surge ζ_1, sway ζ_2, heave ζ_3, roll ζ_4, pitch ζ_5, yaw ζ_6) can be described by a set of second order equations

$$\sum_{k=1}^{6}(M_{j,k}+A_{j,k})\frac{d^2\zeta_k}{dt^2}+B_{j,k}\frac{d\zeta_k}{dt}+C_{j,k}\zeta_k=F_j \qquad j=1,2,\ldots 6,$$

where M is the generalised mass matrix, A and B are the added-mass and damping coefficient matrix, C is the hydrostatic coefficient matrix and F is exciting force and

moment vector. In the derivation of these equations using strip theory [1], it is assumed that motions are small. Not only is the free-surface boundary condition linearised about the undisturbed water surface, but also is the body boundary condition expanded about the mean position. For large-amplitude motions in the severe seas, the influence of the varying underwater part of the hull will be significant, so this linearisation of body boundary condition may not be justified. To rectify this weakness, a coupled time and frequency domain method is presented in this paper from the engineering practice point of view. A fully time-domain method is **not** adopted, because it requires the evaluation of convolution integrals over all previous time steps. This may cause strip theory to loose its numerical simplicity over other methods. At each time step, the exact submerged part of each section is extracted, hydrodynamic coefficients and forces are then calculated based on this instantaneous body boundary. Therefore, at each time instant, the equations of ship motions still keep as simple form as the above equations, but the $M_{j,k}$, $A_{j,k}$, $B_{j,k}$, $C_{j,k}$ and F_j are varying.

2 THE BOUNDARY-VALUE PROBLEM

For a real ship in a seaway, the fluid domain is effectively unbounded relative to the scale of the ship. Figure 1 depicts the geometry and coordinate system of this fluid domain used in the computation. V represents the fluid volume bounded above by the free surface S_f and body surface S_b, below by the sea bed surface S_h, and at the infinity by a enclosing contour S_∞. $\vec{n}$ is the unit normal vector of the boundary surface pointing out of the fluid domain. A right-handed coordinate system $\bar{o}(\bar{x}, \bar{y}, \bar{z})$ is fixed in space. The $\bar{x}, \bar{y}$-plane lies in the still water surface. The still water surface is the average water surface level or surface of the water if no wave were present; $\bar{x}$-axis is directed as the ship mean forward speed; $\bar{z}$-axis points vertically down.

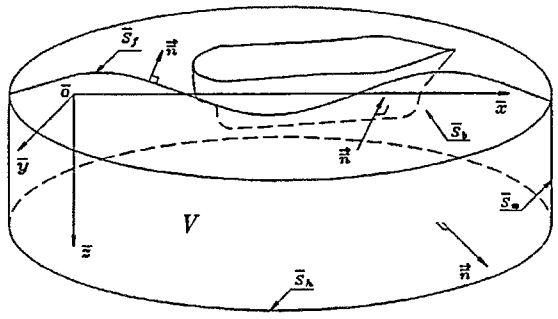

Figure 1: Boundary Value Problem

Suppose now a ship is moving horizontally with constant forward speed U through a harmonic wave. Let $o(x, y, z)$ be a right-handed coordinate system moving in the same direction as the ship with speed U, with x, y-plane lying in the still water surface, x pointing in the direction of ship forward speed and z pointing vertically down as shown in Figure 2. The third coordinate system $o'(x', y', z')$ is fixed to the ship and its origin is situated at the ship's centre of gravity. In the calm water, the ship's centre of gravity is located at $(0, 0, -H_G)$ with respect to the coordinate system $o(x, y, z)$, x' is in the longitudinal forward direction, y' is in the lateral starboard side direction, and z' is vertically down.

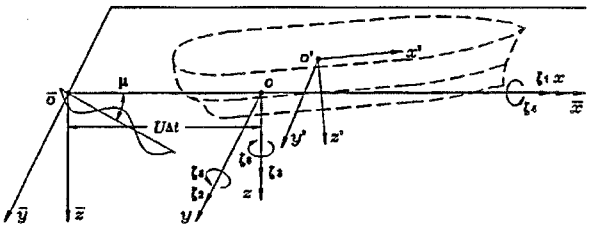

Figure 2: Coordinate System

Initially, the $o(x, y, z)$ coordinate system is coincident with the earth fixed system $\bar{o}(\bar{x}, \bar{y}, \bar{z})$, however after a time Δt, it has moved a distance $U\,\Delta t$ from $\bar{o}$ along the $\bar{x}$-axis.

Within the coordinate system $\bar{o}(\bar{x}, \bar{y}, \bar{z})$, the incident harmonic wave is defined to have a wavelength λ, an amplitude η_0, and a heading angle of μ relative to the $\bar{x}$-axis ($\mu = 0$ for following waves).

The ship is supposed to carry out oscillations around the translating $o(x, y, z)$ coordinate system, which may be described by the translational motions surge ζ_1, sway ζ_2, and heave ζ_3, and rotational motions roll ζ_4, pitch ζ_5, and yaw ζ_6.

Assuming that the fluid is inviscid, incompressible, the fluid flow motion may be described using potential theory. By defining a scalar fluid velocity potential $\bar{\phi}$, the continuity equation reduces to Laplace's equation and the momentum equations reduce to Bernoulli's equation. Therefore, the governing equations are,

$$\nabla^2\bar{\phi}(\vec{\bar{x}}, t) = 0 \qquad \vec{\bar{x}} \in V, \qquad (1)$$

$$\frac{\partial\bar{\phi}}{\partial t} + \frac{1}{2}(\nabla\bar{\phi})^2 + \frac{\bar{p}}{\rho} - g\bar{z} = 0 \qquad \vec{\bar{x}} \in V. \qquad (2)$$

with this formulation, the potential $\bar{\phi}$ and pressure $\bar{p}$ are uncoupled. Typically a solution for $\bar{\phi}$ is found by satisfying (1) along with appropriate boundary conditions. Then, $\bar{p}$ is easily computed using (2).

On the ship hull, the velocity potential $\bar{\phi}$ must satisfy the boundary condition,

$$\frac{\partial\bar{\phi}}{\partial\bar{n}} = \nabla\bar{\phi}\cdot\vec{n} = \vec{\bar{V}}_b(\vec{\bar{x}})\cdot\vec{n} \qquad \vec{\bar{x}} \in \bar{S}_b, \qquad (3)$$

where $\vec{\bar{V}}_b(\vec{\bar{x}})$ is the velocity of the points on the ship hull. On the sea bottom surface the boundary condition is,

$$\frac{\partial\bar{\phi}}{\partial\bar{n}} = \nabla\bar{\phi}\cdot\vec{n} = 0 \qquad \vec{\bar{x}} \in \bar{S}_h. \qquad (4)$$

Suppose the free surface $\bar{S}_f$ is defined by its elevation $\bar{z} = \bar{\eta}(\bar{x}, \bar{y}, t)$, then on this surface, the velocity potential must satisfy the boundary condition,

$$\frac{\partial^2 \bar{\phi}}{\partial t^2} + 2\nabla\bar{\phi}\cdot\nabla\Big(\frac{\partial\bar{\phi}}{\partial t}\Big) + \frac{1}{2}\nabla\bar{\phi}\cdot\nabla(\nabla\bar{\phi}\cdot\nabla\bar{\phi}) - g\frac{\partial\bar{\phi}}{\partial\bar{z}} = 0 \qquad \vec{\bar{x}} \in \bar{S}_f. \quad (5)$$

In addition, a radiation condition is required at infinity to guarantee a unique solution of this boundary value problem.

It is usually more convenient to carry out the calculation in the steady-moving system $o(x, y, z)$. By the Lorentz transformation, Equation (1)-(5) can be written as,

$$\nabla^2\phi(\vec{x}, t) = 0 \qquad \vec{x} \in V, \quad (6)$$

$$\frac{\partial\phi}{\partial t} - U\frac{\partial\phi}{\partial x} + \frac{1}{2}(\nabla\phi)^2 + \frac{p}{\rho} - gz = 0 \qquad \vec{x} \in V, \quad (7)$$

$$\frac{\partial\phi}{\partial n} = \nabla\phi\cdot\vec{n} = [U\vec{e}_1 + \dot{\vec{\alpha}}(\vec{x})]\cdot\vec{n} \qquad \vec{x} \in S_b, \quad (8)$$

$$\frac{\partial\phi}{\partial n} = \nabla\phi\cdot\vec{n} = 0 \qquad \vec{x} \in S_h, \quad (9)$$

$$\frac{\partial^2\phi}{\partial t^2} - 2U\frac{\partial^2\phi}{\partial x\partial t} + U^2\frac{\partial^2\phi}{\partial x^2} + 2\nabla\phi\cdot\nabla\Big(\frac{\partial\phi}{\partial t} - U\frac{\partial\phi}{\partial x}\Big) - g\frac{\partial\phi}{\partial z} + \frac{1}{2}\nabla\phi\cdot\nabla(\nabla\phi)^2 = 0 \qquad \vec{x} \in S_f. \quad (10)$$

where $\vec{\alpha}(\vec{x})$ is the oscillatory displacement of ship hull relative to the coordinate system $o(x, y, z)$ and $\dot{\vec{\alpha}}(\vec{x})$ is the oscillatory speed, $\vec{n}$ is the unit normal vector defined same as $\vec{\bar{n}}$ but related to the coordinate system $o(x, y, z)$ and free surface S_f is defined by its elevation $z = \eta(x, y, t)$.

Once the pressure of the fluid is obtained, the force and moment acting on the ship hull can be calculated by integrating the pressure over the ship hull surface S_b,

$$\vec{F} = [F_1, F_2, F_3] = \iint_{S_b} p\vec{n}ds, \quad (11)$$

$$\vec{M} = [F_4, F_5, F_6] = \iint_{S_b} p(\vec{x}\times\vec{n})ds. \quad (12)$$

3 THE LINEARISED PROBLEM

To solve the velocity potential ϕ with the nonlinear boundary conditions (8)–(10) is rather difficult. In most of the cases, they must be linearised.

The wave potential ϕ is assumed to be the sum of the steady wave potential component ϕ_S and the unsteady component ϕ_T,

$$\phi(\vec{x}, t) = \phi_S(\vec{x}) + \phi_T(\vec{x}, t) \quad (13)$$

ϕ_S is the steady state flow potential due to the ship's forward motion without the presence of incident waves. ϕ_T is unsteady flow potential associated with oscillatory motion of the ship in the incident waves. The geometry of the hull is assumed to be such that the steady state potential ϕ_S and its derivatives are small. The oscillatory motions of the ship are also assumed to be small, so that the unsteady potential ϕ_T and its derivatives are small. Substituting $\phi(\vec{x}, t)$ and $\phi_S(\vec{x})$ into (8) and (10) respectively (hereafter, the water depth is assumed to be infinity, hence, the boundary condition (9) is no longer necessary.), neglecting the higher-order terms of ϕ_S and ϕ_T, and applying Taylor expansions about the mean-hull position S_{bs} in the hull boundary condition and about the undisturbed free surface $z = 0$ in the free surface boundary condition, it can be shown that ϕ_S and ϕ_T must satisfy the following linear boundary conditions:

for ϕ_S,

$$\frac{\partial\phi_S}{\partial n} = U\vec{e}_1\cdot\vec{n} \qquad \vec{x} \in S_{bs}, \quad (14)$$

$$U^2\frac{\partial^2\phi_S}{\partial x^2} - g\frac{\partial\phi_S}{\partial z} = 0 \qquad \vec{x} \in z = 0, \quad (15)$$

for ϕ_T,

$$\frac{\partial\phi_T}{\partial n} = \{\dot{\alpha} + \nabla\times[\alpha\times\nabla(-Ux + \phi_S)]\}\cdot\vec{n} \qquad \vec{x} \in S_{bs}, \quad (16)$$

$$\frac{\partial^2\phi_T}{\partial t^2} - 2U\frac{\partial^2\phi_T}{\partial x\partial t} + U^2\frac{\partial^2\phi_T}{\partial x^2} - g\frac{\partial\phi_T}{\partial z} = 0 \qquad \vec{x} \in z = 0. \quad (17)$$

Boundary condition (16) was derived by Timman and Newman [6], $\vec{n}$ is the unit normal vector of the hull surface. Furthermore, with the restriction that the unsteady motions are small and sinusoidal in time with the frequency of encounter ω_e, ϕ_T can be linearly decomposed as [7],

$$\phi_T = \Re\Big[\phi_0 e^{i\omega_e t} + \phi_7 e^{i\omega_e t} + \sum_{j=1}^{6}\zeta_j\phi_j e^{i\omega_e t}\Big], \quad (18)$$

where the ϕ_0 is the incident wave potential, ϕ_7 is the diffraction wave potential, and ϕ_j $(j = 1, 2, \ldots 6)$ are the radiation potentials due to motions of the ship in each of the six degrees of freedom. The potentials must satisfy the following boundary conditions,

$$\frac{\partial\phi_0}{\partial n} + \frac{\partial\phi_7}{\partial n} = 0 \qquad \vec{x} \in S_{bs}, \quad (19)$$

$$\frac{\partial\phi_j}{\partial n} = i\omega_e n_j + Um_j \qquad \vec{x} \in S_{bs},\ j = 1, 2, \ldots 6, \quad (20)$$

$$\Big[\Big(i\omega_e - U\frac{\partial}{\partial x}\Big)^2 - g\frac{\partial}{\partial z}\Big]\phi_j = 0 \qquad \vec{x} \in z = 0,\ j = 0, 1, \ldots 7. \quad (21)$$

Neglecting the steady wave potential ϕ_S in (16), the generalised normal n_j and m_j are defined by,

$$[n_1, n_2, n_3] = \vec{n}, \tag{22}$$
$$[n_4, n_5, n_6] = \vec{x} \times \vec{n} \qquad \vec{x} \in S_{bs}, \tag{23}$$
$$[m_1, m_2, m_3] = \vec{0}, \tag{24}$$
$$[m_4, m_5, m_6] = [0, n_3, -n_2]. \tag{25}$$

From equation (20), the radiation potentials ϕ_j ($j = 1, 2, \ldots 6$) can be further linearly separated into a speed-independent part ϕ_j^0 and a speed-dependent part ϕ_j^u,

$$\phi_j = \phi_j^0 + \frac{U}{i\omega_e}\phi_j^u \qquad j = 1, 2, \ldots 6. \tag{26}$$

ϕ_j^0 and ϕ_j^u satisfy the boundary conditions (21) on the free surface, and on the ship hull surface, they must satisfy the boundary conditions,

$$\frac{\partial \phi_j^0}{\partial n} = \omega_e n_j \qquad j = 1, 2, \ldots 6, \tag{27}$$
$$\frac{\partial \phi_j^u}{\partial n} = \omega_e m_j \qquad j = 1, 2, \ldots 6, \tag{28}$$

which show the potentials $\phi_j^u = 0$ ($j = 1, 2, 3, 4$), $\phi_5^u = \phi_3^0$ and $\phi_6^u = -\phi_2^0$, thus,

$$\phi_j = \phi_j^0 \qquad j = 1, 2, 3, 4, \tag{29}$$
$$\phi_5 = \phi_5^0 + \frac{U}{\omega_e}\phi_3^0, \tag{30}$$
$$\phi_6 = \phi_6^0 - \frac{U}{\omega_e}\phi_2^0. \tag{31}$$

Neglecting the high-order terms in the Bernoulli's equation, now the force and moment exerted on the ship hull surface (11) and (12) can be evaluated as,

$$\begin{aligned} F_j &= -\rho \iint_{S_{bs}} \Big(\frac{\partial \phi}{\partial t} - U\frac{\partial \phi}{\partial x} - gz\Big) n_j ds \\ &= \Re(F_j^I + F_j^D + F_j^R + F_j^S) \quad j = 1, 2, \ldots 6, \end{aligned} \tag{32}$$

where,

$$F_j^I = -\rho e^{i\omega_e t} \iint_{S_{bs}} \Big(i\omega_e \phi_0 - U\frac{\partial \phi_0}{\partial x}\Big) n_j ds, \tag{33}$$
$$F_j^D = -\rho e^{i\omega_e t} \iint_{S_{bs}} \Big(i\omega_e \phi_7 - U\frac{\partial \phi_7}{\partial x}\Big) n_j ds, \tag{34}$$
$$F_j^R = -\rho e^{i\omega_e t} \iint_{S_{bs}} \sum_{k=1}^{6} \zeta_k \Big(i\omega_e \phi_k - U\frac{\partial \phi_k}{\partial x}\Big) n_j ds, \tag{35}$$
$$F_j^S = \rho g \iint_{S_b} z n_j ds. \tag{36}$$

4 RADIATION FORCES

The detail of calculating hydrodynamics force F_j^R can be found in Salvesen, *et al.* [1]. In summary, it can be expressed as,

$$\begin{aligned} F_j^R &= \sum_{k=1}^{6} \zeta_k e^{i\omega_e t} \Big[-\rho \iint_{S_{bs}} \Big(i\omega_e \phi_k - U\frac{\partial \phi_k}{\partial x}\Big) n_j ds\Big] \\ &= \sum_{k=1}^{6} \zeta_k e^{i\omega_e t} \Big[-i\omega_e \rho \iint_{S_{bs}} \phi_k n_j ds \\ &\quad + U\rho \iint_{S_{bs}} \phi_k m_j ds - U\rho \int_{L_{ca}} \phi_k n_j dl\Big] \\ &= \sum_{k=1}^{6} (\omega_e^2 A_{j,k} - i\omega_e B_{j,k}) \zeta_k e^{i\omega_e t}, \end{aligned} \tag{37}$$

where L_{ca} refers to the underwater girth of the aftermost cross section C_a of the ship, $A_{j,k}$ and $B_{j,k}$ are given by,

i. for $j = 1, 2, 3, 4$

$$A_{j,k} = \int_{L_s} a_{j,k} dx - \frac{U}{\omega_e^2} b_{j,k}^a \quad k = 1, 2, 3, 4, \tag{38}$$
$$B_{j,k} = \int_{L_s} b_{j,k} dx + U a_{j,k}^a \quad k = 1, 2, 3, 4, \tag{39}$$
$$\begin{aligned} A_{j,5} &= -\int_{L_s} x a_{j,3} dx - \frac{U}{\omega_e^2} \int_{L_s} b_{j,3} dx \\ &\quad + \frac{U}{\omega_e^2} x_a b_{j,3}^a - \frac{U^2}{\omega_e^2} a_{j,3}^a, \end{aligned} \tag{40}$$
$$\begin{aligned} B_{j,5} &= -\int_{L_s} x b_{j,3} dx + U \int_{L_s} a_{j,3} dx \\ &\quad - U x_a a_{j,3}^a - \frac{U^2}{\omega_e^2} b_{j,3}^a, \end{aligned} \tag{41}$$
$$\begin{aligned} A_{j,6} &= \int_{L_s} x a_{j,2} dx + \frac{U}{\omega_e^2} \int_{L_s} b_{j,2} dx \\ &\quad - \frac{U}{\omega_e^2} x_a b_{j,2}^a + \frac{U^2}{\omega_e^2} a_{j,2}^a, \end{aligned} \tag{42}$$
$$\begin{aligned} B_{j,6} &= \int_{L_s} x b_{j,2} dx - U \int_{L_s} a_{j,2} dx \\ &\quad + U x_a a_{j,2}^a + \frac{U^2}{\omega_e^2} b_{j,2}^a, \end{aligned} \tag{43}$$

ii. for $j = 5, 6$

$$\begin{aligned} A_{5,k} &= -\int_{L_s} x a_{3,k} dx + \frac{U}{\omega_e^2} \int_{L_s} b_{3,k} dx \\ &\quad + \frac{U}{\omega_e^2} x_a b_{3,k}^a \quad k = 1, 2, 3, 4, \end{aligned} \tag{44}$$
$$\begin{aligned} B_{5,k} &= -\int_{L_s} x b_{3,k} dx - U \int_{L_s} a_{3,k} dx \\ &\quad - U x_a a_{3,k}^a \quad k = 1, 2, 3, 4, \end{aligned} \tag{45}$$

$$A_{5,5} = \int_{L_s} x^2 a_{3,3} dx + \frac{U^2}{\omega_e^2} \int_{L_s} a_{3,3} dx - \frac{U}{\omega_e^2} x_a^2 b_{3,3}^a + \frac{U^2}{\omega_e^2} x_a a_{3,3}^a, \quad (46)$$

$$B_{5,5} = \int_{L_s} x^2 b_{3,3} dx + \frac{U^2}{\omega_e^2} \int_{L_s} b_{3,3} dx + U x_a^2 a_{3,3}^a + \frac{U^2}{\omega_e^2} x_a b_{3,3}^a, \quad (47)$$

$$A_{5,6} = -\int_{L_s} x^2 a_{3,2} dx - \frac{U^2}{\omega_e^2} \int_{L_s} a_{3,2} dx + \frac{U}{\omega_e^2} x_a^2 b_{3,2}^a - \frac{U^2}{\omega_e^2} x_a a_{3,2}^a, \quad (48)$$

$$B_{5,6} = -\int_{L_s} x^2 b_{3,2} dx - \frac{U^2}{\omega_e^2} \int_{L_s} b_{3,2} dx - U x_a^2 a_{3,2}^a - \frac{U^2}{\omega_e^2} x_a b_{3,2}^a, \quad (49)$$

$$A_{6,k} = \int_{L_s} x a_{2,k} dx - \frac{U}{\omega_e^2} \int_{L_s} b_{2,k} dx - \frac{U}{\omega_e^2} x_a b_{2,k}^a \quad k = 1,2,3,4, \quad (50)$$

$$B_{6,k} = \int_{L_s} x b_{2,k} dx + U \int_{L_s} a_{2,k} dx + U x_a a_{2,k}^a \quad k = 1,2,3,4, \quad (51)$$

$$A_{6,5} = -\int_{L_s} x^2 a_{2,3} dx - \frac{U^2}{\omega_e^2} \int_{L_s} a_{2,3} dx + \frac{U}{\omega_e^2} x_a^2 b_{2,3}^a - \frac{U^2}{\omega_e^2} x_a a_{2,3}^a, \quad (52)$$

$$B_{6,5} = -\int_{L_s} x^2 b_{2,3} dx - \frac{U^2}{\omega_e^2} \int_{L_s} b_{2,3} dx - U x_a^2 a_{2,3}^a - \frac{U^2}{\omega_e^2} x_a b_{2,3}^a, \quad (53)$$

$$A_{6,6} = \int_{L_s} x^2 a_{2,2} dx + \frac{U^2}{\omega_e^2} \int_{L_s} a_{2,2} dx - \frac{U}{\omega_e^2} x_a^2 b_{2,2}^a + \frac{U^2}{\omega_e^2} x_a a_{2,2}^a, \quad (54)$$

$$B_{6,6} = \int_{L_s} x^2 b_{2,2} dx + \frac{U^2}{\omega_e^2} \int_{L_s} b_{2,2} dx + U x_a^2 a_{2,2}^a + \frac{U^2}{\omega_e^2} x_a b_{2,2}^a. \quad (55)$$

It is worth writing out the critical 'strip theory' assumptions which are used while deriving the radiation forces (37). Firstly, the ship is assumed to be long and slender, so that the surface integrals of ϕ_k^0 implicitly included in (37) can be evaluated as,

$$-\imath\rho\omega_e \iint_{S_b} \phi_k^0 n_j ds = \int_{L_s} \left(-\imath\rho\omega_e \int_{L_{cx}} \phi_k^0 n_j dl \right) dx, \quad (56)$$

where L_s is the ship length, L_{cx} is the underwater girth of the cross section C_x. Secondly, if the ship is long and slender, in the neighbourhood region of the hull, it can be found that $\partial/\partial y \gg \partial/\partial x$, $\partial/\partial z \gg \partial/\partial x$ and $n_2 \gg n_1$, $n_3 \gg n_1$. This means the three-dimensional generalised normal n_j $(j = 2,3,4)$ on the right hand side of (56) can be replaced by the two-dimensional generalised normal $\hat{n}_j$ $(j = 2,3,4)$ in the y,z-plane of the cross section, meanwhile $n_1 \approx 0$, $n_5 \approx -x\hat{n}_3$, and $n_6 \approx x\hat{n}_2$. Finally, the frequency of encounter limitation is assumed to be defined by $\omega_e \gg U(\partial/\partial x)$. This requires that the wave length is approximately of the same order as the ship beam. Under these assumptions the Laplace equation and the boundary conditions (20) and (27) to be satisfied by ϕ_k^0 $(k = 2,3,4)$ reduce to the two-dimensional problem at each given cross section C_x. Let $\hat{\phi}_2 e^{\imath\omega_e t}$, $\hat{\phi}_3 e^{\imath\omega_e t}$, and $\hat{\phi}_4 e^{\imath\omega_e t}$ be the two-dimensional potentials due to the unit motion of sway, heave, and roll, respectively, of a cylinder with cross section C_x oscillating with the frequency ω_e in the free surface. Therefore, $\phi_1^0 \approx 0$, $\phi_k^0 \approx \hat{\phi}_k$ $(k = 2,3,4)$, and from the boundary condition (27), $\phi_5^0 \approx -x\hat{\phi}_3$, $\phi_6^0 \approx x\hat{\phi}_2$. $\hat{\phi}_k(y,z)$ $(k = 2,3,4)$ must satisfy the Laplace equation and the boundary conditions as follows,

$$\frac{\partial \hat{\phi}_k}{\partial \hat{n}} = \imath\omega_e \hat{n}_k \qquad (y,z) \in L_{cx}, k = 2,3,4, \quad (57)$$

$$\omega_e^2 \hat{\phi}_k + g\frac{\partial \hat{\phi}_k}{\partial z} = 0 \quad (y,z) \in z = 0, k = 2,3,4, \quad (58)$$

$$g\frac{\partial \hat{\phi}_k}{\partial y} \pm \imath\omega_e^2 \hat{\phi}_k = 0 \quad y \to \pm\infty, k = 2,3,4. \quad (59)$$

It is now clear that the radiation forces (37) eventually is the function of the integrals,

$$-\imath\omega_e\rho \int_{L_{cx}} \hat{\phi}_k \hat{n}_j dl = \omega_e^2 a_{j,k} - \imath\omega_e b_{j,k} \quad j,k = 2,3,4, \quad (60)$$

which exactly are the two-dimensional hydrodynamic forces on the cross section C_x, thus $a_{j,k}$ and $b_{j,k}$ are the corresponding two-dimensional added mass and damping coefficients. $a_{j,k}^a$ and $b_{j,k}^a$ refer to the added mass and damping coefficients of the aftermost section C_a.

5 EXCITING FORCES

Using linear gravity-wave theory, the potential for a incident plane-progressive wave of amplitude η_0 satisfying the boundary condition (58) is given by,

$$\phi_0 = \frac{ig\eta_0}{\omega_0} e^{-K_0(z + \imath x\cos\mu - \imath y\sin\mu)}, \quad (61)$$

where μ is the heading angle, $K_0 = 2\pi/\lambda$ is the wave number, λ is the wave length, and $\omega_0 = \sqrt{gK_0}$ is the wave frequency, which is related to the frequency of encounter ω_e by,

$$\omega_e = \omega_0 - K_0 U\cos\mu. \quad (62)$$

The exciting forces F_j^I and F_j^D can be calculated in the similar way as that of the radiation forces [1]. Using the

same 'strip theory' assumptions, from (33), (34), (61), and the boundary condition (19), the total exciting forces F_j^E are given by,

$$F_j^E = F_j^I + F_j^D$$
$$= \begin{cases} \rho\eta_0 e^{\imath w_e t}\Big[\int_{L_s}(f_j^I + f_j^D)dx + \dfrac{U}{w_e}f_j^{Da}\Big] \\ \qquad\qquad j = 2,3,4, \\ -\rho\eta_0 e^{\imath w_e t}\Big[\int_{L_s}(xf_3^I + xf_3^D + \dfrac{U}{w_e}f_3^{Da})dx \\ \qquad + \dfrac{U}{w_e}x_a f_3^{Da}\Big] \quad j = 5, \\ \rho\eta_0 e^{\imath w_e t}\Big[\int_{L_s}(xf_2^I + xf_2^D + \dfrac{U}{w_e}f_2^{Da})dx \\ \qquad + \dfrac{U}{w_e}x_a f_2^{Da}\Big] \quad j = 6, \end{cases} \tag{63}$$

where f_j^I is the sectional incident wave force, f_j^D is the sectional diffraction force, and given by,

$$f_j^I = ge^{-\imath xK_0\cos\mu}\int_{L_{cx}}\hat{n}_j e^{K_0(\imath y\sin\mu - z)}dl, \tag{64}$$

$$f_j^D = \omega_0 e^{-\imath xK_0\cos\mu}\int_{L_{cx}}(\imath\hat{n}_3 - \hat{n}_2\sin\mu) \times e^{K_0(\imath y\sin\mu - z)}\hat{\phi}_j dl. \tag{65}$$

Here, f_j^{Da} refers to f_j^D evaluated at the aftermost section C_a.

6 TWO DIMENSIONAL HYDRODYNAMIC FORCES

Ursell [31, 32] derived a potential flow solution, which satisfies the boundary conditions (57)–(59), for a circular cylinder oscillating harmonically with arbitrary frequency in the free surface. Eatock and Hu [33] gave a generalised version of Ursell's solution, which can be applied to both floating and submerged bodies. For a cylinder with arbitrary cross section, the potential solution can be got by conformal transformation techniques.

Westlike and Wilson [34] developed a conformal mapping which can transform an arbitrary section in the physical y, z-plane to a unit circle in the reference plane,

$$y = \mathcal{Y}(r,\theta) = a\Big\{r\sin\theta + \sum_{n=0}^{N}(-1)^n\Big[\frac{a_{2n}}{r^{2n}}\cos 2n\theta + \frac{a_{2n+1}}{r^{2n+1}}\sin(2n+1)\theta\Big]\Big\}, \tag{66}$$

$$z = \mathcal{Z}(r,\theta) = a\Big\{r\cos\theta + \sum_{n=0}^{N}(-1)^n\Big[\frac{a_{2n}}{r^{2n}}\sin 2n\theta - \frac{a_{2n+1}}{r^{2n+1}}\cos(2n+1)\theta\Big]\Big\}. \tag{67}$$

The coefficients a, a_{2n}, a_{2n+1} are determined by,

$$y_p = a\Big\{\sin\theta_p + \sum_{n=0}^{N}(-1)^n[a_{2n}\cos 2n\theta_p + a_{2n+1}\sin(2n+1)\theta_p]\Big\}, \tag{68}$$

$$z_p = a\Big\{\cos\theta_p + \sum_{n=0}^{N}(-1)^n[a_{2n}\sin 2n\theta_p - a_{2n+1}\cos(2n+1)\theta_p]\Big\}, \tag{69}$$

where (y_p, z_p) $(p = 1,2,\ldots,N_p)$ are the offset points representing the boundary of the section in y, z-plane, and $(1,\theta_P)$ are the corresponding mapped points in the reference plane. Therefore, the boundary conditions (57)-(59) are transformed to,

$$\frac{\partial\hat{\phi}_k}{\partial r} = w_e\hat{n}_k \qquad r = 1, \theta\in[-\frac{\pi}{2},\frac{\pi}{2}], k = 2,3,4, \tag{70}$$

$$\omega_e^2\Big(\frac{\partial\mathcal{Z}}{\partial\theta}\Big)_{\theta=\pm\frac{\pi}{2}}\hat{\phi}_k + g\frac{\partial\hat{\phi}_k}{\partial\theta} = 0 \qquad \theta = \pm\frac{\pi}{2}, k = 2,3,4, \tag{71}$$

$$g\frac{\partial\hat{\phi}_k}{\partial r} \pm w_e^2\Big(\frac{\partial\mathcal{Y}}{\partial r}\Big)_{r=\pm\infty}\hat{\phi}_k = 0 \qquad r\to\pm\infty, k = 2,3,4. \tag{72}$$

Similar to the method Ursell used for a semi-immersed circular cylinder, the velocity potential for the case of an arbitrary cross section is also composed of a source potential, a dipole potential and a series of linear multipole potentials,

$$\hat{\phi}_k = P_{k,0}\varphi_0 + P_{k,1}\varphi_1 + \sum_{m=1}^{\infty}(P_{k,2m}\varphi_{2m} + P_{k,2m+1}\varphi_{2m+1}), \tag{73}$$

where,

$$\varphi_0 = \int_0^\infty \frac{K_e\sin(\beta\mathcal{Z}) - \beta\cos(\beta\mathcal{Z})}{K_e^2+\beta^2}e^{-\beta|\mathcal{Y}|}d\beta + \imath\pi e^{-K_e(\mathcal{Z}+\imath|\mathcal{Y}|)}, \tag{74}$$

$$\varphi_1 = \mp\int_0^\infty \frac{K_e\cos(\beta\mathcal{Z}) + \beta\sin(\beta\mathcal{Z})}{K_e^2+\beta^2}e^{-\beta|\mathcal{Y}|}d\beta \pm \pi e^{-K_e(\mathcal{Z}+\imath|\mathcal{Y}|)} + \frac{\mathcal{Y}}{K_e(\mathcal{Y}^2+\mathcal{Z}^2)} \quad \mathcal{Y}\gtrless 0, \tag{75}$$

$$\varphi_{2m} = \frac{\cos(2m\theta)}{r^{2m}} + aK_e\Big\{\frac{\cos[(2m-1)\theta]}{(2m-1)r^{2m-1}} - \sum_{n=0}^{N}(-1)^n\Big[2na_{2n}\frac{\sin[(2m+2n)\theta]}{(2m+2n)r^{2m+2n}} - (2n+1)a_{2n+1}\frac{\cos[(2m+2n+1)\theta]}{(2m+2n+1)r^{2m+2n+1}}\Big]\Big\}, \quad (76)$$

$$\varphi_{2m+1} = \frac{\sin[(2m+1)\theta]}{r^{2m+1}} + aK_e\Big\{\frac{\sin(2m\theta)}{2mr^{2m}} + \sum_{n=0}^{N}(-1)^n\Big[2na_{2n}\frac{\cos[(2m+2n+1)\theta]}{(2m+2n+1)r^{2m+2n+1}} + (2n+1)a_{2n+1}\frac{\sin[(2m+2n+2)\theta]}{(2m+2n+2)r^{2m+2n+2}}\Big]\Big\}. \quad (77)$$

All the potentials satisfy the Laplace's equation, and the boundary conditions (71)(72, the unknown constants $P_{k,0}$, $P_{k,1}$, $P_{k,2m}$, $P_{k,2m+1}$ are chosen in the way such that the boundary condition (70) is satisfied.

7 SHIP MOTION EQUATIONS

If the ship is considered as a rigid body, with respect to the coordinate system $o(x,y,z)$, its motion now can be determined by,

$$\sum_{k=1}^{6}[M_{j,k}(t) + A_{j,k}(t)]\frac{d^2\zeta_k}{dt^2} + B_{j,k}(t)\frac{d\zeta_k}{dt} = F_j^S(t) + F_j^E(t) + F_j^G(t) \quad j = 1,2,\ldots 6, \quad (78)$$

where $M_{j,k}$ is the generalised mass matrix for the ship,

$$M_{j,k} = \begin{pmatrix} m & 0 & 0 & 0 & mz_G & -my_G \\ 0 & m & 0 & -mz_G & 0 & mx_G \\ 0 & 0 & m & my_G & -mx_G & 0 \\ 0 & -mz_G & my_G & I_{11} & I_{12} & I_{13} \\ mz_G & 0 & -mx_G & I_{21} & I_{22} & I_{23} \\ -my_G & mx_G & 0 & I_{31} & I_{32} & I_{33} \end{pmatrix}, \quad (79)$$

$$F_j^G = [0,0,mg,mgy_G,-mgx_G,0], \quad (80)$$

where m is the mass of the ship, (x_G,y_G,z_G) is the location of centre of gravity at each time step, $I_{j,k}$ are the moments of inertia, and F_j^G are the forces and moments due to the ship's weight. It should be noticed that the S_{b_s} used to derive the strip theory refers to the wetted hull surface at the mean position. However, in the present method, the definition of mean position is different from the conventional strip theory, it refers to the instantaneous wetted hull surface at each time step. Hence, F_j^S can be calculated on the surface S_{b_s}, instead of S_b in the equation (36).

8 NUMERICAL CALCULATION & RESULTS

The hull form chosen to test this numerical model was a frigate, which has already been used by Westlake and Wilson [2]. The main particulars are shown in Table (1) and the rationalised twenty-one equally spaced body plans are presented in Figure (3). In order to simplify the calculation, the sections are extrapolated to the maximum depth of the ship, and the phantom offsets above the deck are added. The number of waterlines must be enough to secure the accuracy when calculating the wetted sections. In the present calculation fifty waterlines are used (ten of them are shown in Figure (3)). The waterlines are not equally spaced, but closer to the keel are more concentrated.

Particulars	Data
Length	130.0 m
Mass Displacement	4248.0 tonnes
Draught	4.722 m
Beam	8.10 m
LCG (aft of the stem head)	75.5 m
VCG (above the baseline)	6.05 m
Trim Angle (at 15 knots)	1.029 degree

Table 1: Frigate Main Particulars

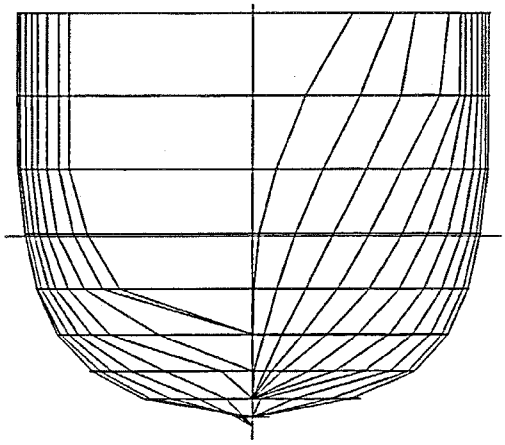

Figure 3: Hull Form

It is found that the number of conformal mapping parameters greatly affects computation time. The time taken to finish mapping one section almost doubles when the parameter number increases 30%. For some complicated sections, such as the section with bilge keels and the section with shaft brackets, the parameters may be as many as 40~50 [34]. The number of conformal mapping parameters is set to be 20 in the present computation, because this frigate hull form is relatively simple. Twenty parameters already can give sufficient accuracy, one sample is shown in Figure (4).

The equations of motions (78) are solved using the Newmark β time stepping method. The time step Δt is 1 second. Initially, the ship is assumed to be advancing with steady speed U, and the pitch, roll, and yaw angle are all 0°. Westlake and Wilson [2] have given some numerical

results, which have been compared with the results provided by a seakeeping suite PAT. PAT was developed by DERA and has been tested by the model scale experiments in oblique regular waves. In their work, the force due to the diffraction wave potential was omitted, but it now is included. Therefore, the comparison with PAT will not be repeated here, only the comparisons with the results produced by Westlake and Wilson are presented.

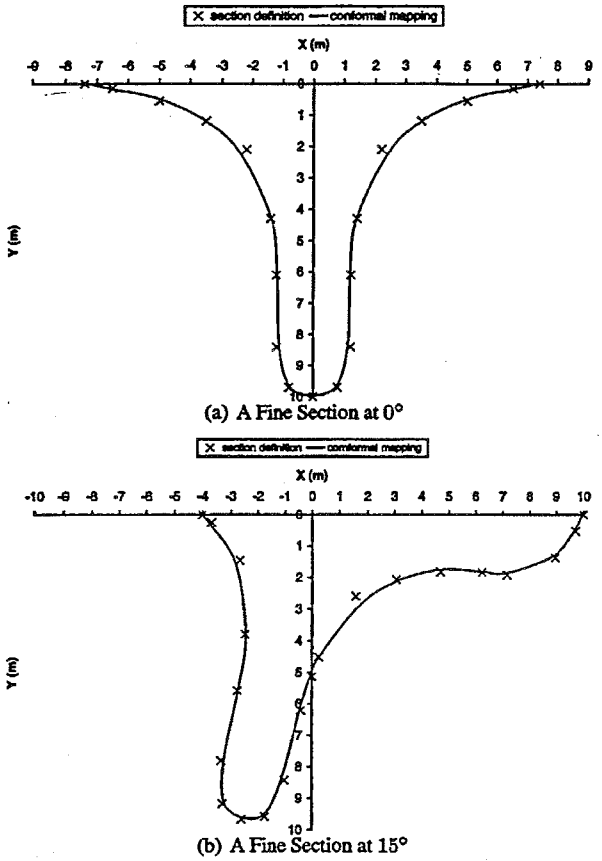

(a) A Fine Section at 0°

(b) A Fine Section at 15°

Figure 4: Sample of Conformal Mapping with 20 Parameters

8.1 SYMMETRIC MOTIONS

Figure (5) and (6) show the heave and pitch motion history in head sea and oblique sea ($\mu = 15°$) respectively. The results are non-dimensionalised using the wave slope amplitude. Cubic splines are used to fit adjacent points, so that the phase relationships between displacement, velocity, and acceleration can be clearly displayed. A wave with length λ of 150 metres and steepness H/λ of 0.00667 is selected for the calculation. The ship's speed is assumed to be 10 knots. The predictions of heave and pitch motion are quite good in terms of the phasing of the motions. The acceleration leads the velocity about $\pi/2$, whilst the displacement lags the velocity about $\pi/2$. It seems that the transient period is short, the motions reach the steady oscillatory state after one and half cycle. The reason may be because the time convolution term is omitted in the equations of motions, so that the initial condition can not effectively affect the motions afterwards.

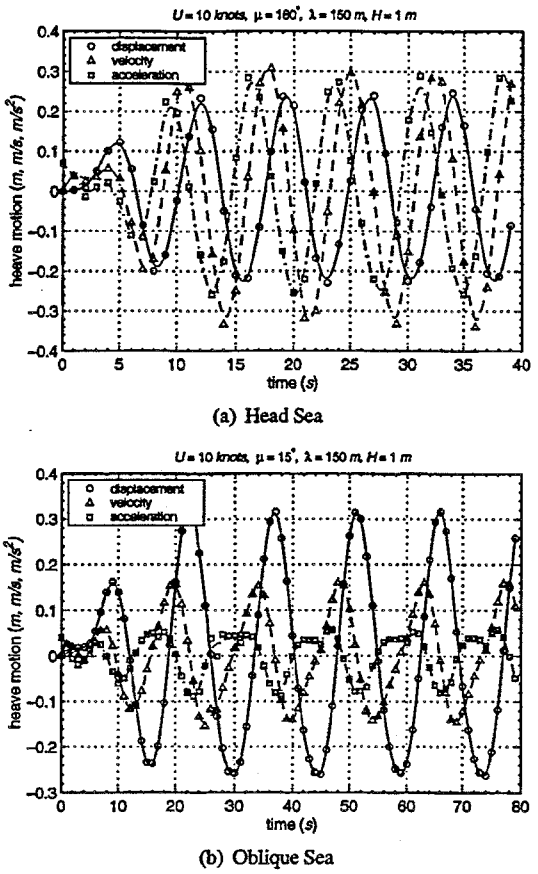

(a) Head Sea

(b) Oblique Sea

Figure 5: Heave Motion in Head Sea and Oblique Sea

The change of ship advance speed directly results in the change of frequency of encounter ω_e. Figure (7) and (8) show the comparison of displacement, velocity and acceleration of heave motion at speed 10, 15, and 20 knots in the head sea. Wave length λ is still 150 metres and wave amplitude H is 1 metre. The frequencies ω_e of encounter, therefore, are 0.86 rad/s, 0.96 rad/s, and 1.07 rad/s respectively. The corresponding periods T are 7.3 s, 6.5 s, and 5.9 s, which are depicted very accurately in the graph. This also further proves that the time stepping scheme is correct. It can be found that the amplitude of the heave motion decreases as the ship speed increases, while the tendency of pitch amplitude is not very clear. The same fact can be found in the results produced by program PAT in the range $\omega_e \approx 0.8 \sim 1.2$ rad/s [2].

8.2 ANTI-SYMMETRIC MOTIONS

The predictions of anti-symmetric motions in the time domain seem quite problematic. One of the important reasons is the lack of restoring forces for the sway and yaw

motions. Small perturbations in these motions will result in the ship being deviated from its original course. For a ship advancing in oblique sea (heading angle $\mu = 15°$), this process is clearly illustrated in Figure (9). The displacements of both sway and yaw tend to diverge quickly, however the velocity and acceleration still can keep relatively stable. The drift of yaw motion result in the change of heading angle. If there are no means to correct this false action, the program eventually will malfunction. Application of a virtual rudder moment might be a effective method, and is currently being researched.

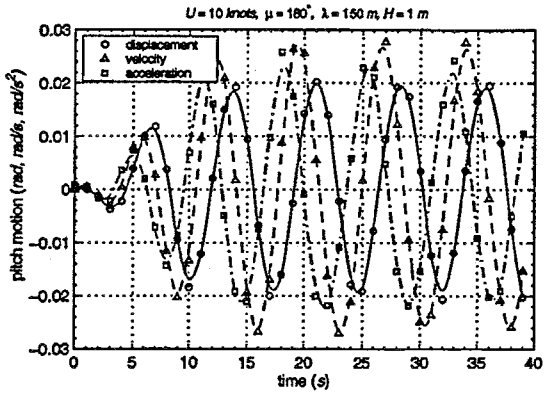

(a) Head Sea

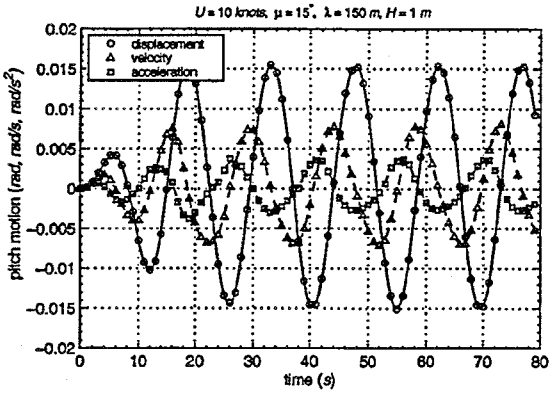

(b) Oblique Sea

Figure 6: Pitch Motion in Head Sea and Oblique Sea

Salvesen, *et al* [1] pointed out that, in the case of sway, yaw and roll motion, the added-mass and damping coefficients are significantly affected by viscosity, especially the roll-damping coefficient $B_{4,4}$ even in the absence of bilge keels. Hence, the necessary correction of roll-damping coefficient must be made to take account for the viscous effect. However, it needs an iterative computational process which is difficult to implement in the time stepping scheme. So the roll motion shown in the Figure (10) is computed with un-corrected roll-damping coefficient. Undoubtedly, the prediction does not agree well with the real fact and can not reach steady oscillatory state. In addition, it is also deteriorated by yaw drift, in other words, by the accumulation of heading angle change.

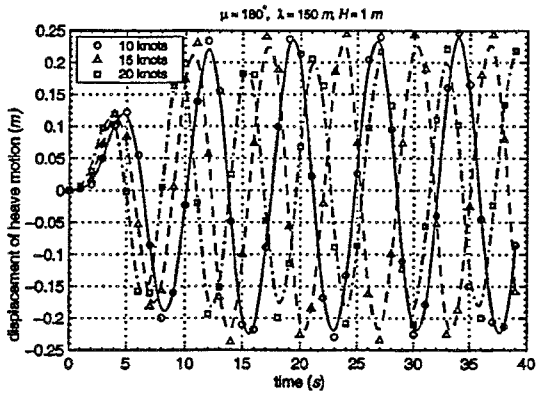

(a) Displacement of Heave Motion

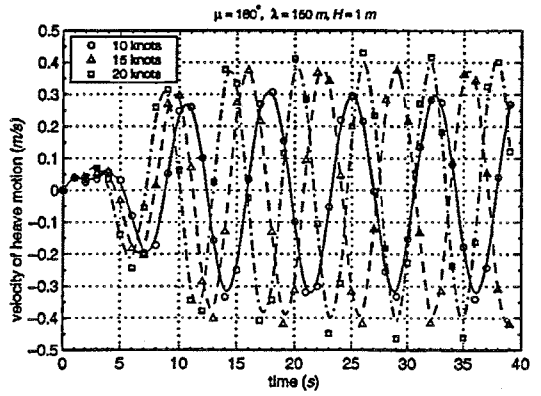

(b) Velocity of Heave Motion

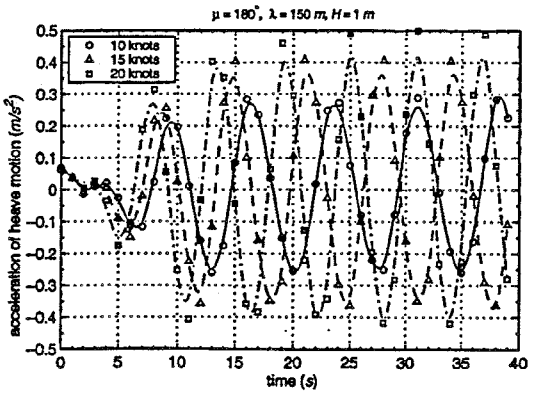

(c) Acceleration of Heave Motion

Figure 7: Comparison of Heave Motions with Different Speeds

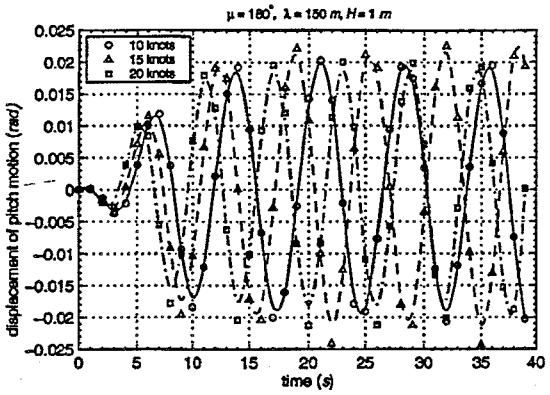

(a) Displacement of Pitch Motion

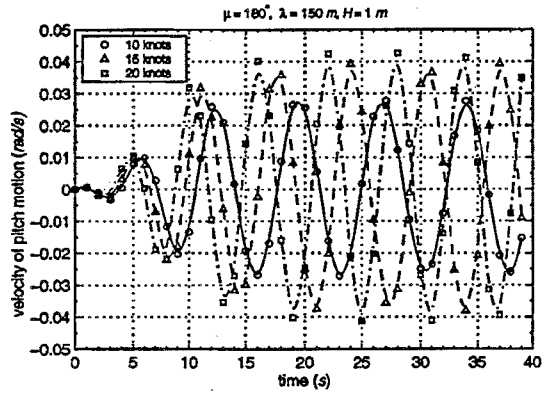

(b) Velocity of Pitch Motion

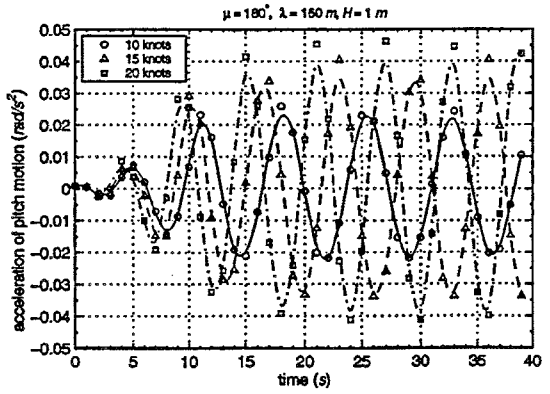

(c) Acceleration of Pitch Motion

Figure 8: Comparison of Pitch Motions with Different Speeds

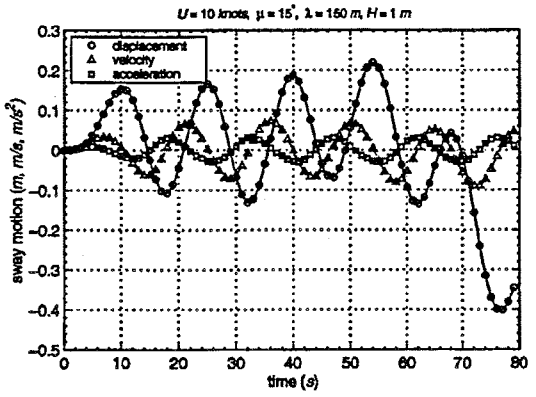

(a) Sway Motion

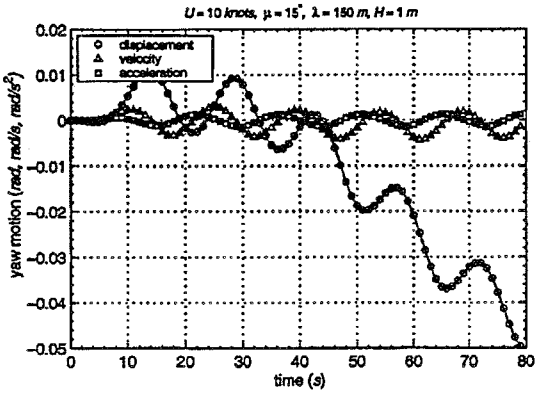

(b) Yaw Motion

Figure 9: Sway and Yaw Motion in Oblique Sea

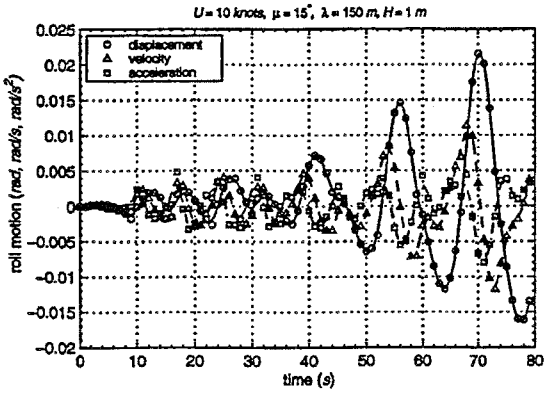

Figure 10: Roll Motion in Oblique Sea

8.3 EFFECT OF DIFFRACTION FORCE

Comparisons of displacement, velocity, and acceleration for the heave and pitch motion in head sea between the cases with and without diffraction force are shown in Figure (11) and (12). The amplitudes of both heave and pitch motion are increased about 25% when the diffraction is added. Therefore, the effect of diffraction force is significant and should not be neglected. Adding the diffraction has no influence on the phasing of the motions and transient process which is still relatively short.

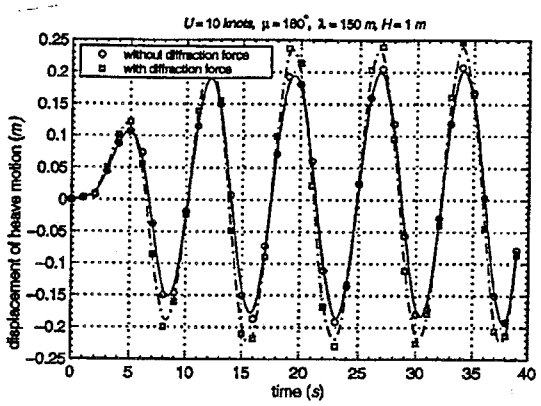

(a) Displacement of Heave Motion

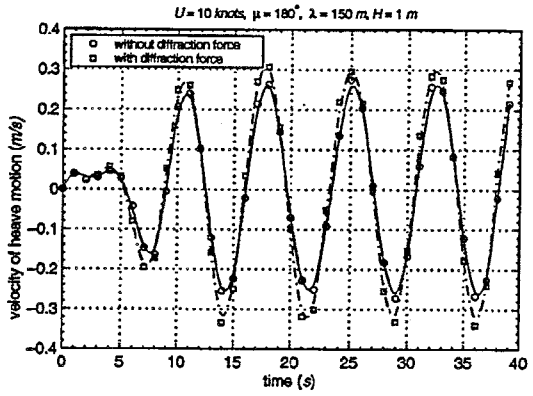

(b) Velocity of Heave Motion

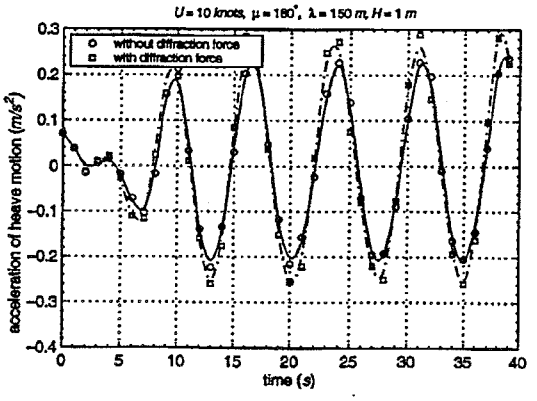

(c) Acceleration of Heave Motion

Figure 11: Effect of Diffraction Force on Heave Motion

8.4 COMPARISON WITH SERIES 60 HULL ECPERIMENTAL DATA

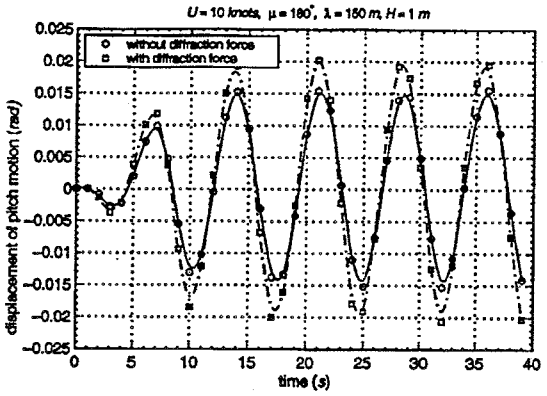

(a) Displacement of Pitch Motion

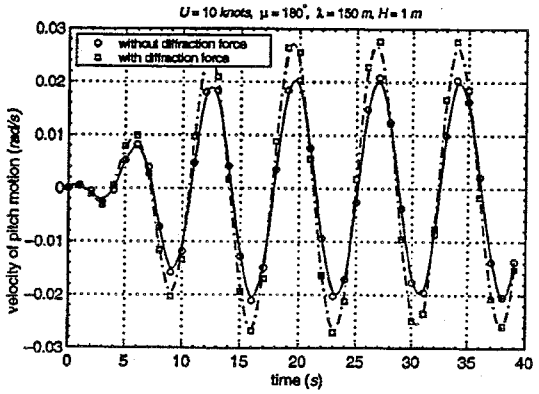

(b) Velocity of Pitch Motion

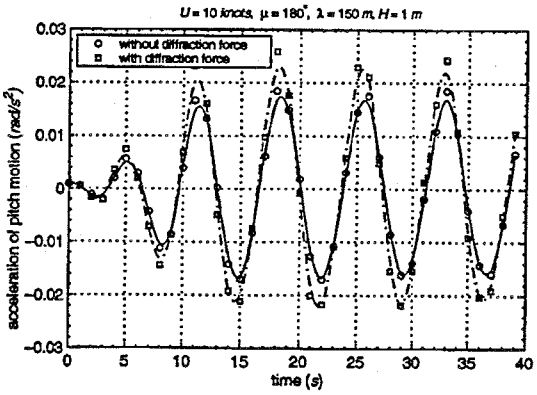

(c) Acceleration of Pitch Motion

Figure 12: Effect of Diffraction Force on Pitch Motion

Here the series 60 hull form is chosen to validate this time domain method, because it has been extensively studied numerically and experimentally and a large amount of data is available. Since the the anti-symmetric motions are not well predicted at this moment, as pointed out in last section, only the validations of heave and pitch motions are presented hereafter. Figure (13(a)) and Figure (13(b)) show the comparisons of pitch and heave motion RAOs of a Series 60 ($C_b = 0.70$) ship model travelling at

a Froude number of 0.2 in regular head waves. The experimental data were given by Gerritsma and Beukelman[35]. The computational results of three-dimensional frequency

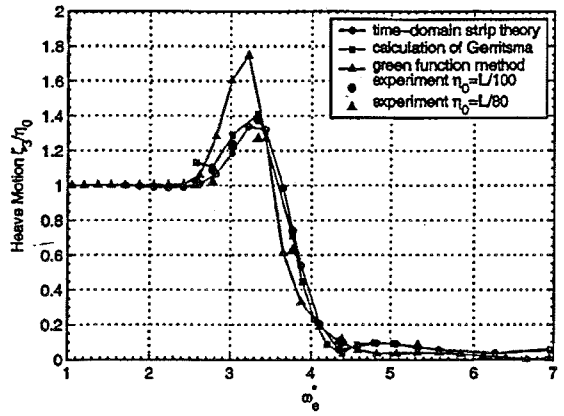

(a) Heave Motion

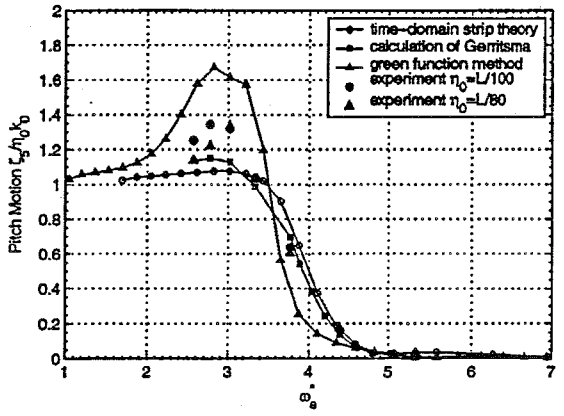

(b) Pitch Motion

Figure 13: Comparison of Heave and Pitch Motion ($\eta_0 = 0.01016, Fn = 0.2$)

domain Green function method [36] using 510 panels are also illustrated. ω_e^* is the non-dimensionalised frequency of encounter, $\omega_e^* = \omega_e * \sqrt{gL}$, where L is the ship length between perpendiculars. Comparisons show that theoretical results and experimental data are in reasonable close agreement. It is clear that the three dimensional Green function method always over-predicts around the resonant frequency. However, Strip theory tends to under-predict, especially for pitch motion. The results of time domain strip theory method ($\eta_0 = L/300$) are very close to the computational results given by Gerritsma and Beukelman [35].

As the incident wave amplitude η_0 increases, slight difference near resonance frequency appears in both heave and pitch motion RAOs, which can be seen in Figure (14(a)) and Figure (14(b)). The difference is not significant, but it clearly shows the non-linear effect of varying underwater surface, and it is believed this phenomenon will be more significant as the wave amplitude increases more.

9 CONCLUSIONS

This paper is complementary to the work by Westlake and Wilson [2] who developed the basic frame of this time-domain non-linear strip theory. The diffraction force omitted by Westlake and Wilson now has been added, and its influence has been demonstrated in this paper. The results show that the diffraction force have an important effect.

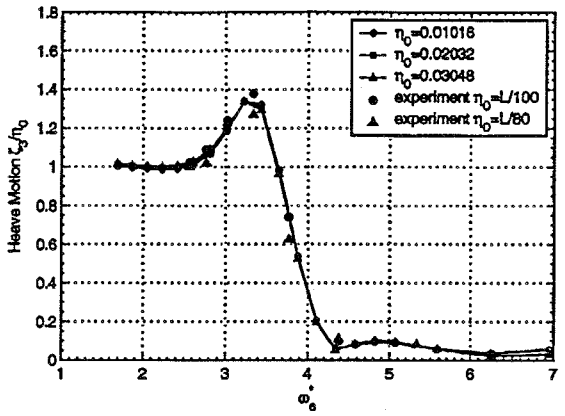

(a) Heave Motion

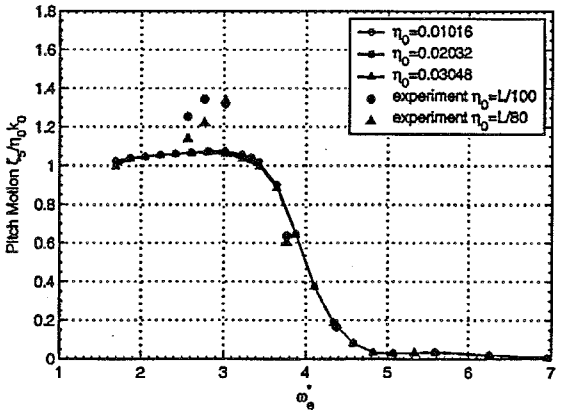

(b) Pitch Motion

Figure 14: Effect of Wave Amplitude ($F_n = 0.2$)

The feasibility of extending linear strip theory to deal with large-amplitude motions by encompassing the changing shape of the wetted hull has been tested again. The hydrodynamic coefficients and forces are not entirely linear because the wetted hull surface varies with time. The results obtained so far are quite encouraging in the sense of comparison with the results from linear strip theory program.

However, the predictions of anti-symmetric motions in oblique seas are not yet effective. The methods for inhibiting sway and yaw drift need to be developed, as well as the methods for correcting the roll-damping coefficient in time domain. In addition, since the eventual aim of this work is to predict the large-amplitude motions of a ship in

large seaway, the free surface elevation might not be negligible. The influence of free surface elevation on wetted surface now is being investigated.

References

[1] Salvesen, N., Tuck, E. O., and Faltinsen, O. Ship motions and sea loads. *Transactions of the Society of Naval Architects and Marine Engineers*, 78:250–287, 1970.

[2] Westlake, P. C., Wilson, P. A., and Bailey, P. A. Time domain simulation of ship motions. *Transactions of the Royal Institution of Naval Architects*, 142:57–76, 2000.

[3] Froude, W. The rolling of ships. *Transactions of the Institution of Naval Architects*, 2:180–229, 1861.

[4] Kriloff, C. A. A new theory of the pitching motion of ships on waves, and of the stresses produced by this motion. *Transactions of the Institution of Naval Architects*, 37:326–368, 1896.

[5] Korvin-Kroukovsky, B. V. Investigation of ship motions in regular waves. *Transactions of the Society of Naval Architects and Marine Engineers*, 63:386–435, 1955.

[6] Timman, R. and Newman, J. N. The coupled damping coefficients of symmetric ships. *Journal of Ship Research*, 5(4):1–7, 1962.

[7] Newman, J. N. The theory of ship motions. *Advances in Applied Mechanics*, 18:221–283, 1978.

[8] Newman, J. N. and Sclavounos, P. The unified theory of ship motions. In *Proceedings of 13th Symposium on Naval Hydrodynamics*, pages 373–394, Tokyo, October 1980.

[9] Sclavounos, P. D. The diffraction of free-surface waves by a slender ship. *Journal of Ship Research*, 28(1):29–47, 1984.

[10] Kashiwagi, M., Mizokami, A., Yasukawa, H., and Fukushima, Y. Prediction of wave pressure and loads on actual ships by the enhanced unifed theory. In *Proceedings of 23rd Symposium on Naval Hydrodynamics*, pages 368–384, Val de Reuil, France, September 2000.

[11] Chang, M. S. Computations of three-dimesional ship-motions with forward speed. In *Proceedings of 2nd International Conference on Numerical Ship Hydrodynamics*, pages 124–135, Berkeley, USA, September 1977.

[12] Inglis, R. B. and Price, W. G. A three dimensional ship motion theory – comparison between theoretical predictions and experiment data of the hydrodynamic coefficients with forward speed. *Transactions of the Royal Institution of Naval Architects*, 124:141–157, 1982.

[13] Inglis, R. B. and Price, W. G. A three dimensional ship motion theory: Calculation of wave loading and resopnses with forward speed. *Transactions of the Royal Institution of Naval Architects*, 124:183–192, 1982.

[14] Wu, G. X. and Taylor, R. E. The numerical solution of the motions of a ship advancing in waves. In *Proceedings of 5th International Conference on Numerical Ship Hydrodynamics*, pages 529–538, Hiroshima, Japan, September 1989.

[15] Chen, X. B., Diebold, L., and Doutreleau, Y. New green-function method to predict wave-induced ship motions and loads. In *Proceedings of 23rd Symposium on Naval Hydrodynamics*, pages 66–81, Val de Reuil, France, September 2000.

[16] Dawson, C. W. A practical computer method for solving ship-wave problems. In *Proceedings of 2nd International Conference on Numerical Ship Hydrodynamics*, pages 124–135, Berkeley, USA, September 1977.

[17] Nakos, D. and Sclavounos, P. Ship motions by a three-dimensional rankine panel method. In *Proceedings of 18th Symposium on Naval Hydrodynamics*, pages 21–40, Ann Arbor, Michigan, August 1990.

[18] Nakos, D. and Sclavounos, P. On steady and unsteady ship wave patterns. *Journal of Fluid Mechanics*, 215:263–288, 1990.

[19] Finkelstein, A. B. The initial value problem for transient water waves. *Communications on Pure and Applied Mathematics*, 10(4):511–522, 1957.

[20] Wehausen, J. V. The motion of floating bodies. *Annual Review of Fluid Mechanics*, 3:237–268, 1971.

[21] Yeung, R. W. The transient heaving motion of floating cylinders. *Journal of Engineering Mathematics*, 16(2):97–119, 1982.

[22] Newman, J. N. Transient axisymmetric motion of a floating cylinder. *Journal of Fluid Mechanics*, 157:17–33, 1985.

[23] Beck, R. F. and Liapis, S. Transient motions of floating bodies at zero foward speed. *Journal of Ship Research*, 31(3):164–176, 1987.

[24] King, B. K., Beck, R. F., and Magee, A. R. Seakeeping calculations with forward speed using time-domain analysis. In *Proceedings of 17th Symposium on Naval Hydrodynamics*, pages 577–596, Hague, Netherlands, August - September 1988.

[25] Nakos, D. E., Kring, D., and Scalvounos, P. D. Rankine panel methods for transient free-surface flows. In *Proceedings of 6th International Conference on Numerical Ship Hydrodynamics*, pages 613–632, Iowa City, USA, August 1993.

[26] Lin, W. M. and Yue, D. Numerical solutions for large-amplitude ship motions in the time domain. In *Proceedings of 18th Symposium on Naval Hydrodynamics*, pages 41–66, Ann Arbor, Michigan, August 1990.

[27] Kring, D., Huang, Y. F., Sclavounos, P., Vada, T., and Braathen, A. Nonlinear ship motions and wave-induced loads by a rankine method. In *Proceedings of 21th Symposium on Naval Hydrodynamics*, pages 45–63, Trondheim, Norway, June 1996.

[28] Sclavounos, P. D., Kring, D. C., Huang, Y., Mantzaris, D. A., kim, S., and Kim, Y. A computational method as an advanced tool of ship hydrodynamic design. *Transactions of the Society of Naval Architects and Marine Engineers*, 105:375–397, 1997.

[29] Huang, Y. and Scalvounos, P. D. Nonlinear ship motions. *Journal of Ship Research*, 42(2):120–130, 1998.

[30] Beck, R. and Reed, A. Modern seakeeping computations for ships. In *Proceedings of 23rd Symposium on Naval Hydrodynamics*, pages 1–45, Val de Reuil, France, September 2000.

[31] Ursell, F. On the heaving motion of a circular cylinder on the surface of a fluid. *Quarterly Journal of Mechanics and Applied Mathematics*, 2(2):218–231, 1949.

[32] Ursell, F. On the rolling motion of cylinders in the surface of a fluid. *Quarterly Journal of Mechanics and Applied Mathematics*, 2(3):335–353, 1949.

[33] Taylor, R. E. and Hu, C. S. Multipole expansions for wave diffraction and radiation in deep water. *Ocean Engineering*, 18(3):191–224, 1991.

[34] Westlake, P. C. and Wilson, P. A. A new conformal mapping technique for ship sections. *International Shipbuilding Progress*, 47(449):5–22, 2000.

[35] Gerritsma, J. and Beukelman, W. Comparison of calculated and measured heaving and pitching motions of a series 60, $c_B = 0.70$ ship model in regular longitudinal waves. In *Proceedings of 11th International Towing Tank Conference*, pages 436–442, Tokyo, Japan, October 1966.

[36] Hudson, D. A. *A Validation Study on Mathematical Models of Speed and Frequency Dependence in Seakeeping of High Speed Craft*. PhD thesis, School of Engineering Sciences, University of Southampton, UK, 1999.